

Interaction of Thiourea Derivatives with a C-Steel Surface: Towards the Development of 'Green' Corrosion Inhibitors: Theoretical and Experimental Study

A.M. Eldesoky^{1*}

^{1*} Engineering Chemistry Department, High Institute of Engineering & Technology (New Damietta), Egypt and Al-Qunfudah Center for Scientific Research (QCSR), Al-Qunfudah University College, Umm Al-Qura University, KSA.

E-mail: a.m.eldesoky@hotmail.com

Abstract- The protection influence of three thiourea derivatives against C- steel corrosion was studied in 1 M HCl solutions at 30°C. Measurements were conducted under various experimental conditions using weight loss, potentiodynamic polarization, electrochemical impedance spectroscopy (EIS) and electrochemical frequency modulation (EFM) techniques. These studies have shown that thiourea derivatives are very good "green", mixed-type inhibitors. Electrochemical frequency modulation (EFM) and electrochemical impedance spectroscopy (EIS) method of analysis are also presented here for monitoring corrosion. Corrosion rates obtained from both EFM and EIS methods are comparable with those recorded using Tafel extrapolation method, confirming validation of corrosion rates measured by the latter. The inhibitive action of these thiourea derivatives was discussed in terms of blocking the electrode surface by adsorption of the molecules through the active centers contained in their structures following Temkin adsorption isotherm. Quantum chemical method was also employed to explore the relationship between the inhibitor molecular properties and its protection efficiency. The density function theory (DFT) is used to study the structural properties of thiourea derivatives. The protection efficiencies of these compounds showed a certain relationship to highest occupied molecular orbital (HOMO) energy, Mulliken atomic charges and Fukui indices. The morphology of inhibited and uninhibited C-steel was analyzed by scanning electron microscope (SEM) and energy dispersive X-ray spectroscopy (EDX).

Keywords— C-steel, HCl, EFM, EIS, SEM-EDX, Mulliken atomic charges, Fukui indices.

1 INTRODUCTION C- steel has been extensively used under different conditions in petroleum industries [1]. Aqueous solutions of acids are among the most corrosive media and are widely used in industries for pickling, acid cleaning of boilers, descaling and oil well [2, 6]. The main problem concerning C- steel applications is its relatively low corrosion resistance in acidic solution. Several methods used currently to reduce corrosion of C- steel. One of such methods is the use of organic inhibitors [7-17]. Effective inhibitors are heterocyclic compounds that have π bonds, heteroatoms such as sulphur, oxygen and nitrogen [18]. Compounds containing both nitrogen and chloro atoms can provide excellent inhibition, compared with compounds containing only nitrogen or chloro atom [19]. Heterocyclic compounds such as Thiourea derivatives can provide excellent inhibition. These molecules depends mainly on certain physical properties of the inhibitor molecules such as functional groups, steric factors, electron density at the donor atom and electronic structure of the molecules [20, 21]. Regarding the adsorption of the inhibitor on

the metal surface, two types of interactions are responsible. One is physical adsorption which involves electrostatic force between ionic charges or dipoles of the adsorbed species and electric charge at metal/solution interface. Other is chemical adsorption, which involves charge sharing or charge transfer from inhibitor molecules to the metal surface to form coordinated types of bonds [22]. The selection of appropriate inhibitors mainly depends on the type of acid, its concentration, and temperature.

The objective of the present investigation is to study the corrosion inhibition of C- steel in 1 M HCl using thiourea derivatives and to propose a suitable mechanism for the inhibition process. SEM and EDX examination of the C-steel in 1 M HCl surface revealed that these compounds prevented C-steel in 1 M HCl from corrosion by adsorption on its surface to form a protective film and acts as a barrier to corrosive media. It was also the purpose of the present work to discuss the relationship between quantum chemical calculations and experimental protection efficiencies of the tested thiourea derivatives by determining various

quantum chemical parameters. These parameters include the highest occupied molecular orbital (E_{HOMO}) and the lowest unoccupied molecular orbital (E_{LUMO}), the energy difference (ΔE) between E_{HOMO} and E_{LUMO} .

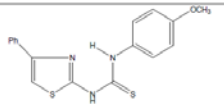
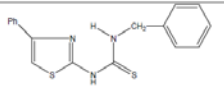
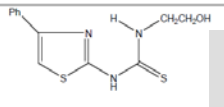
2. EXPERIMENTAL

2.1. Chemicals and Materials

Hydrochloric acid (37%), ethyl alcohol and acetone were purchased from Al-Gomhoria Company. Bidistilled water was used throughout all the experiments.

TABLE (1)

MOLECULAR STRUCTURES, FORMULAS AND MOLECULAR WEIGHTS OF THE INVESTIGATED THIOUREA DERIVATIVES[22].

Comp.	Structures	Names	Mol. Formula Mol. Wt
1		1-(4-methoxyphenyl)-3-(4-phenylthiazol-2-yl)thiourea	$C_{18}H_{15}N_3OS_2$ Mol. Wt: 341.45
2		1-benzyl-3-(4-phenylthiazol-2-yl)thiourea	$C_{18}H_{15}N_3S_2$ Mol. Wt: 325.45
3		1-(2-hydroxyethyl)-3-(4-phenylthiazol-2-yl)thiourea	$C_{16}H_{15}N_3OS_2$ Mol. Wt: 279.38

The composition of C-steel (weight %) is given in Table (2):

TABLE (2)

CHEMICAL COMPOSITION OF C- STEEL (WEIGHT %)

ELEMENT	C	Mn	P	Si	Fe
WEIGHT (%)	0.200	0.350	0.024	0.003	rest

2.2. Methods

2.2.1. Weight Loss Measurements

Rectangular specimens of C-steel with dimensions 2.1 x 2.0 x 0.2 cm were abraded with different grades of emery paper, degreased with acetone, rinsed with bidistilled water and dried between filter papers. After weighting accurately, the specimens were immersed in 100 ml of 1 M HCl with and without different concentrations of inhibitors at 30 °C. After different immersion periods, the C-steel samples were taken out, washed with bidistilled water, dried and weighted again. The weight loss values are used to calculate the corrosion rate (R) in mmy⁻¹ by Eq. (1):

$$R = (\text{weight loss in gram} \times 8.75 \times 10^4) / DAT \quad (1)$$

Where D is C-steel density in g cm⁻³, A is exposed area

in cm², T is exposure time in hr.

The inhibition efficiency (%IE) and the degree of surface coverage (θ) were calculated from Eq. (2):

$$\%IE = \theta \times 100 = [(R^* - R) / R^*] \times 100 \quad (2)$$

Where R^* and R are the corrosion rates of C-steel in the absence and in the presence of inhibitor, respectively.

2.2.2. Electrochemical Measurements

Electrochemical measurements were conducted in a conventional three electrodes thermostated cell assembly using an Gamry potentiostat/galvanostat/ZRA (model PCI300/4). A platinum foil and saturated calomel electrode (SCE) were used as counter and reference electrodes, respectively. The C- steel electrodes were 1x1 cm and were welded from one side to a copper wire used for electrical connection. The electrodes were abraded, degreased and rinsed as described in weight loss measurements. All experiments were carried out at temperature (30 ± 1°C). The potentiodynamic curves were recorded from -500 to 500 mV at a scan rate 1 mV S⁻¹ after the steady state is reached (30 min) and the open circuit potential (OCP) was noted. The % IE and degree of surface coverage were calculated from Eq. (3):

$$IE\% = \theta \times 100 = [1 - (i_{corr}^0 / i_{corr})] \times 100 \quad (3)$$

Where i_{corr}^0 and i_{corr} are the corrosion current densities of uninhibited and inhibited solution, respectively.

Electrochemical impedance spectroscopy (EIS) and electrochemical frequency modulation (EFM) experiments were carried out using the same instrument as before with a Gamry framework system based on ESA400. Gamry applications include software EIS300 for EIS measurements and EFM140 for EFM measurements; computer was used for collecting data. Echem Analyst 5.5 Software was used for plotting, graphing and fitting data. EIS measurements were carried out in a frequency range of 100 kHz to 10 mHz with amplitude of 5 mV peak-to-peak using ac signals at respective corrosion potential. EFM carried out using two frequencies 2 and 5 Hz. The base frequency was 1 Hz. In this study, we use a perturbation signal with amplitude of 10 mV for both perturbation frequencies of 2 and 5 Hz.

2.2.3. SEM-EDX Measurement

The C-steel surface was prepared by keeping the specimens for 3 days immersion in 1 M HCl in the presence and absence of optimum concentrations of investigated derivatives, after abraded using different

emery papers up to 1200 grit size. Then, after this immersion time, the specimens were washed gently with bidistilled water, carefully dried and mounted into the spectrometer without any further treatment. The corroded C-steel surfaces were examined using an X-ray diffractometer Philips (pw-1390) with Cu-tube (Cu Ka1, $\lambda = 1.54051 \text{ \AA}$), a scanning electron microscope (SEM, JOEL, JSM-T20, Japan).

2.2.4. Theoretical Study

Accelrys (Material Studio Version 4.4) software for quantum chemical calculations has been used.

3. RESULTS AND DISCUSSION

3.1. Weight Loss Measurements

Figure (1) shows the weight loss-time curves for the corrosion of C-steel in 1 M HCl in the absence and presence of different concentrations of compound (1). Similar curves for other compounds were obtained and are not shown. The data of Table (3) show that, the inhibition efficiency increases with increase in inhibitor concentration from 11×10^{-6} to 21×10^{-6} M. The maximum inhibition efficiency was achieved at 21×10^{-6} M. The lowest inhibition efficiency (%IE) is obtained in the presence of compound (3), therefore %IE tends to decrease in the following order: compound (1) > compound (2) > compound (3).

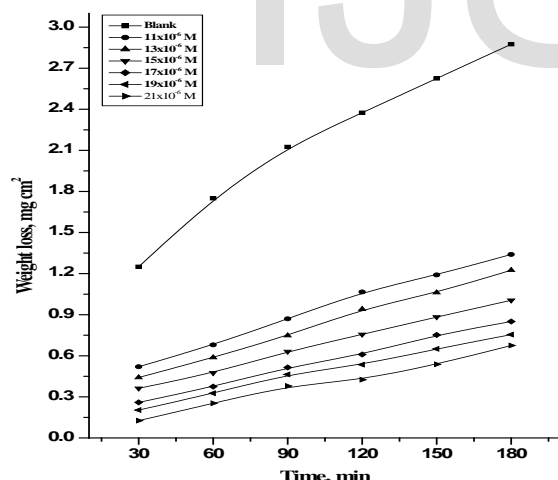


Fig. 1 Weight loss-time curves for C-steel dissolution in 1 M HCl in the absence and presence of different concentrations of inhibitor (1) at 30 °C.

TABLE 3

VARIATION OF INHIBITION EFFICIENCY (%IE) OF DIFFERENT COMPOUNDS WITH THEIR MOLAR CONCENTRATIONS FROM WEIGHT LOSS MEASUREMENTS AT 120 MIN IMMERSION IN 1 M HCl AT 30 °C

Conc. (M)	Inhibition Efficiency (% IE)		
	1	2	3
11×10^{-6}	55.1	44.74	37.37
13×10^{-6}	60.41	50	44.21
15×10^{-6}	68.18	54.21	50.79
17×10^{-6}	74.34	59.52	55.26
19×10^{-6}	77.48	65.4	58.68
21×10^{-6}	82.11	73.17	70.74

3.1.2. Adsorption Isotherm

Assuming the corrosion inhibition was caused by the adsorption of thiourea derivatives, and the values of surface coverage for different concentrations of thiourea derivatives in 1 M HCl were evaluated from weight loss. From the values of (Θ) , it can be seen that these values increased with increasing the concentration of thiourea derivatives. Using these values of surface coverage, one can utilize different adsorption isotherms to deal with experimental data. The Temkin adsorption isotherm was applied to investigate the adsorption mechanism, by plotting (Θ) vs. $\log C$, and straight lines were obtained Fig. (2). On the other hand, it is found that Kinetic-thermodynamic model of El-Awady et al [23] which has the formula:

$$\log (\Theta / 1 - \Theta) = \log K' - y \log C \quad (4)$$

Is valid and verify the present adsorption data Fig. 3. The equilibrium constant of adsorption $K = K'(1/y)$, where $1/y$ is the number of the surface active sites occupied by one organic molecule and C is the bulk concentration of the inhibitor.

The thermodynamic parameters for the adsorption process that were obtained from these Figures are shown in Table (4). The values of $\Delta G^{\circ}_{\text{ads}}$ are negative and increased as the % IE increased which indicate that these investigated thiourea derivatives are strongly adsorbed on the C-steel surface and show the spontaneity of the adsorption process and stability of the adsorbed layer on the C-steel surface. Generally, values of $\Delta G^{\circ}_{\text{ads}}$ up to -20 kJ mol^{-1} are consistent with the electrostatic interaction between the charged molecules and the charged metal (physical adsorption) while those more negative than -40 kJ mol^{-1} involve sharing or transfer of electrons from the inhibitor molecules to the metal surface to form a coordinate

type of bond (chemisorptions) [24]. The values of ΔG°_{ads} obtained were approximately equal to (41.21–56.41) kJ mol⁻¹, indicating that the adsorption mechanism of the thiourea derivatives on C-steel in 1 M HCl solution involves both electrostatic adsorption and chemisorptions [25]. The thermodynamic parameters point toward both physisorption (major contributor) and chemisorptions (minor contributor) of the inhibitors onto the metal surface. The K_{ads} follow the same trend in the sense that large values of K_{ads} imply better more efficient adsorption and hence better inhibition efficiency.

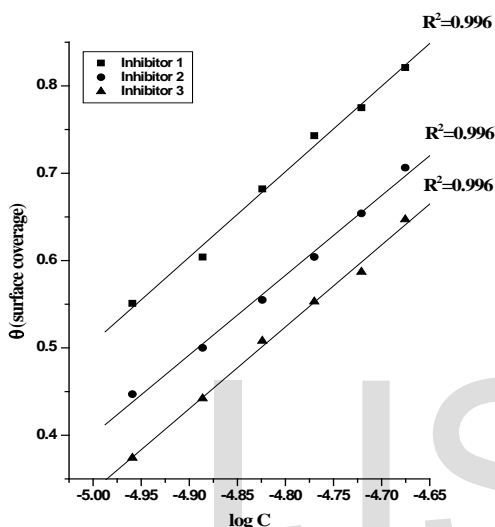


Fig . 2. Curve fitting of corrosion data for C-steel in 1 M HCl in presence of different concentrations of thiourea derivatives to the Temkin adsorption isotherm at 30°C.

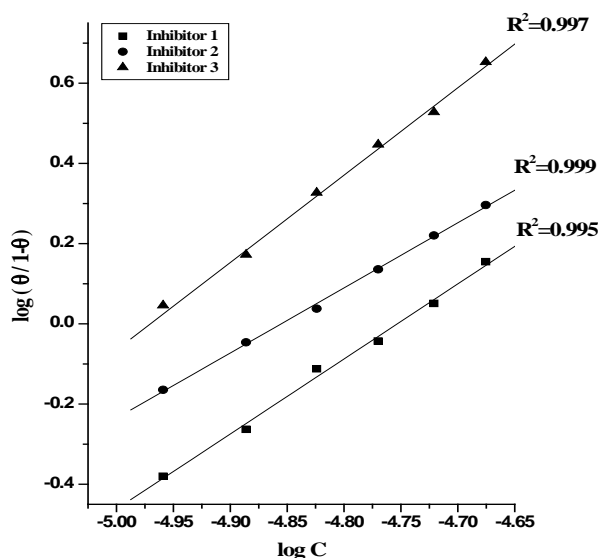


Fig.3. Curve fitting of corrosion data for C-steel in 1 M HCl in presence of different concentrations of thiourea derivatives to the kinetic model at 30°C.

TABLE .4
PARAMETERS OBTAINED FROM TEMKIN ADSORPTION ISOTHERM AND KINETIC MODEL FOR C- STEEL IN 1 M HCL FOR INVESTIGATED THIOUREA DERIVATIVES AT 30°C.

Compound	Temkin			Kinetic model		
	a	K_{ads} M ⁻¹	$-\Delta G^{\circ}_{ads}$ kJ mol ⁻¹	1/y	K_{ads} M ⁻¹	$-\Delta G^{\circ}_{ads}$ kJ mol ⁻¹
1	2.35	328877.0	42.13	0.50	96862.96	56.41
2	2.52	274404.2	41.67	0.57	77231.37	44.07
3	2.45	228398.1	41.21	0.59	67420.32	38.47

3.1.3. Effect of Temperature

The activation energies (E_a) for the corrosion of C-steel in the absence and presence of different concentrations of thiourea derivatives derivatives were calculated using Arrhenius-type Eq [27]:

$$\log k = \log A - E_a / 2.303RT \quad (5)$$

Where A is the pre-exponential factor, k is the rate constant, E_a is the apparent activation energy of the corrosion process, R is the universal gas constant and T is the absolute temperature. Arrhenius plots of log k vs. 1/T for C-steel in 1 M HCl in the absence and presence of different concentration of inhibitors (1) are shown graphically in Fig. 4. The variation of log k vs. 1/T is a linear one and the values of E_a were calculated from the slope of these lines and given in Table 5. The increase in E_a with the addition of concentration of inhibitors (1-3) indicating that the energy barrier for the corrosion reaction increases. It is also indicated that the whole process is controlled by surface reaction, since the activation energy of the corrosion process is larger than 20 kJ mol⁻¹ [28].

Enthalpy and entropy of activation (ΔH^* , ΔS^*) for the corrosion of C- steel in 1 M HCl were obtained by applying the transition state Eq(6):

$$k = (RT/Nh) \exp (\Delta S^*/R) \exp (-\Delta H^*/RT) \quad (6)$$

Where h is Planck's constant, N is Avogadro's number. A plot of log k/T vs 1/T also gave straight lines as shown in Fig. 5 for C-steel dissolution in 1 M HCl in the absence and presence of different concentration of inhibitor (1). The slopes of these lines equal $-\Delta H^*/2.303R$ and the intercept equal $\log RT/Nh + (\Delta S^*/2.303R)$ from which the value of ΔH^* and ΔS^* were calculated and tabulated in Table 5. From these results, it is clear that the presence of the tested compounds increased the activation energy values and consequently decreased the corrosion rate of the C-steel. These results indicate that these tested

compounds acted as inhibitors through increasing activation energy of C-steel dissolution by making a barrier to mass and charge transfer by their adsorption on C-steel surface. Positive sign of the enthalpies reflects the endothermic nature of the C-steel dissolution process.

All values of E_a^* are larger than the analogous values of ΔH^* indicating that the corrosion process must involved a gaseous reaction, simply the hydrogen evolution reaction, associated with a decrease in the total reaction volume [29]. The values of ΔS^* in absence and presence of the tested compounds are large and negative; this indicates that the activated complex in the rate-determining step represents an association rather than dissociation step, meaning that a decrease in disordering takes place on going from reactants to the activated complex [30, 31].

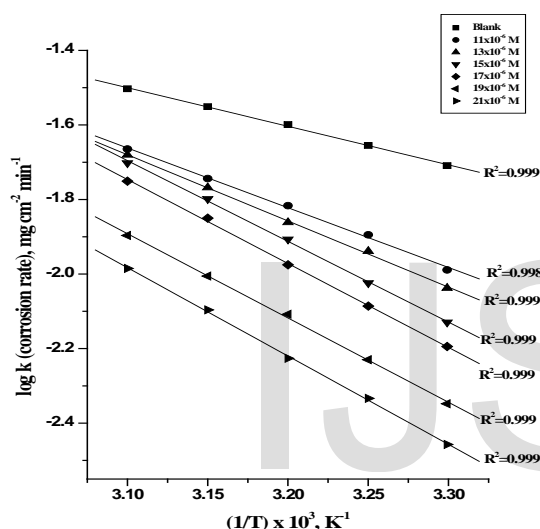


Fig. 4. Arrhenius plots (log k vs 1/T) for C-steel in 1 M HCl in absence and presence of different concentration of inhibitor (1).

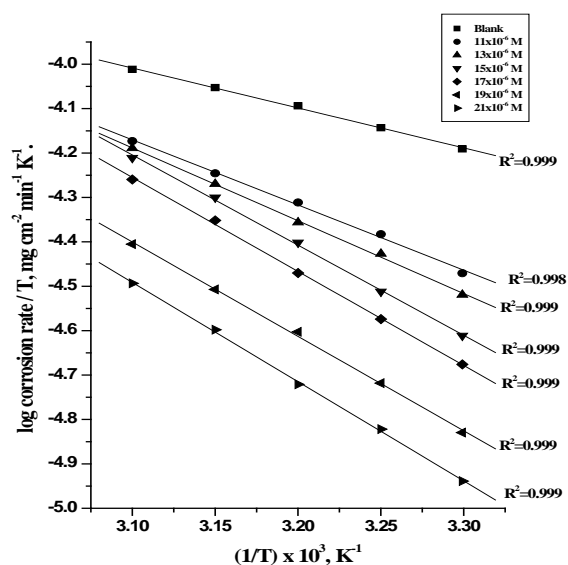


Fig.5 Transition state plots (log k/T vs 1/T) for C-steel in 1 M

HCl in absence and presence of different concentration of Inhibitor (1).

TABLE. 5
ACTIVATION PARAMETERS OF THE DISSOLUTION OF C-STEEL IN 1 M HCL IN THE ABSENCE AND PRESENCE OF DIFFERENT CONCENTRATION OF ORGANIC DERIVATIVE

Inhibitor	Conc., M.	Activation Parameters		
		E_a^* kJ mol ⁻¹	ΔH^* kJ mol ⁻¹	$-\Delta S^*$ J mol ⁻¹ K ⁻¹
Blank	----	10.23	3.31	275.34
Compound (1)	11x10 ⁻⁵	30.71	12.21	198.36
	13x10 ⁻⁵	34.01	13.64	199.72
	15x10 ⁻⁵	41.51	16.89	199.83
	17x10 ⁻⁵	43.15	17.61	204.39
	19x10 ⁻⁵	43.32	17.68	207.64
Compound (2)	21x10 ⁻⁵	45.41	18.59	210.13
	11x10 ⁻⁵	24.26	9.41	204.88
	13x10 ⁻⁵	25.23	9.82	208.81
	15x10 ⁻⁵	26.48	10.37	214.24
	17x10 ⁻⁵	28.19	11.11	219.21
Compound (3)	19x10 ⁻⁵	29.97	11.88	219.91
	21x10 ⁻⁵	30.23	12.00	244.30
	11x10 ⁻⁵	19.38	7.28	205.29
	13x10 ⁻⁵	21.26	8.10	214.77
	15x10 ⁻⁵	23.27	8.98	237.70
	17x10 ⁻⁵	24.08	9.33	239.56
	19x10 ⁻⁵	25.02	9.74	241.83
	21x10 ⁻⁵	26.37	10.32	225.41

3.2. Potentiodynamic Polarization Studies

The cathodic and anodic polarization curves for C-steel in 1 M HCl solution in absence and presence of various concentrations of the inhibitors (1) at 30 °C are shown in Fig.(6). Similar curves were obtained for other inhibitors (not shown). The various electrochemical parameters calculated from Tafel plots are given in Table 6. The lower corrosion current density (i_{corr}) values in presence of the inhibitors without causing significant changes in corrosion potential (E_{corr}) suggest that the investigated compounds are mixed type inhibitors and are adsorbed on the surface thereby blocking the corrosion reaction [32].

The results also show that the slopes of the anodic and the cathodic Tafel slopes (β_a and β_c) were slightly changed on increasing the concentration of the tested compounds. This indicates that there is no change in the mechanism of inhibition in presence and absence

of inhibitors. The values of β_c are slightly higher than the values of β_a suggesting a cathodic action of the inhibitor. The higher values of Tafel slope can be attributed to surface kinetic process rather the diffusion-controlled process [33].

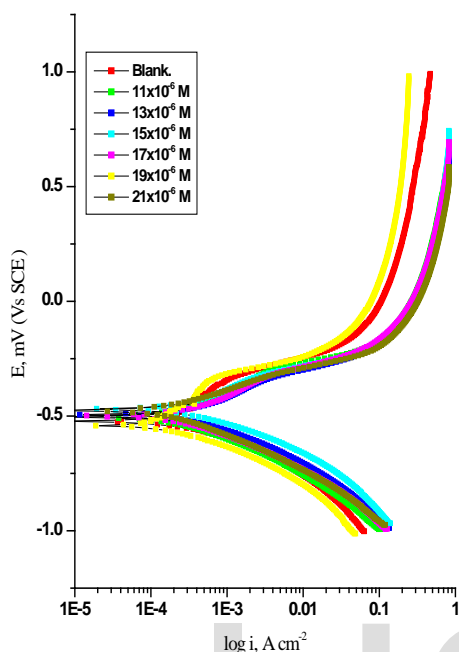


Fig. 6. Potentiodynamic polarization curves for C-steel in 1 M HCl in the absence and presence of different concentrations of inhibitor (1) at 30°C.

TABLE.6

THE EFFECT OF CONCENTRATION OF THE INVESTIGATED COMPOUNDS ON THE FREE CORROSION POTENTIAL (E_{CORR}), CORROSION CURRENT DENSITY (i_{CORR}), TAFEL SLOPES (β_a & β_c), INHIBITION EFFICIENCY (% IE), AND DEGREE OF SURFACE COVERAGE FOR THE CORROSION OF C-STEEL IN 1 M HCL AT 30°C

Comp.	Conc., M.	$-E_{corr} \times 10^{-3}$ mV(vs SCE)	$i_{corr} \times 10^{-4}$ $\mu A \text{ cm}^{-2}$	$\beta_a \times 10^{-4}$ mV dec ⁻¹	$\beta_c \times 10^{-4}$ mV dec ⁻¹	θ	% IE
1	Blank	521	12.000	66	76	---	---
	11 × 10 ⁻⁶	473	0.665	14	67	0.9445	94.45
	13 × 10 ⁻⁶	491	0.632	115	80	0.9473	94.73
	15 × 10 ⁻⁶	489	0.284	64	57	0.9763	97.63
	17 × 10 ⁻⁶	516	0.232	73	51	0.9806	98.06
	19 × 10 ⁻⁶	484	0.231	78	78	0.9807	98.07
	21 × 10 ⁻⁶	469	0.160	82	47	0.9866	98.66
2	11 × 10 ⁻⁶	559	1.580	110	117	0.8683	86.83
	13 × 10 ⁻⁶	489	1.230	116	103	0.8975	89.75
	15 × 10 ⁻⁶	483	1.100	28	90	0.9083	90.83
	17 × 10 ⁻⁶	460	0.875	142	83	0.9270	92.70
	19 × 10 ⁻⁶	492	0.870	16	78	0.9275	92.75
	21 × 10 ⁻⁶	507	0.864	16	79	0.9280	92.80
3	11 × 10 ⁻⁶	503	9.100	39	10	0.2416	24.16
	13 × 10 ⁻⁶	493	8.39	26	38	0.3008	30.08
	15 × 10 ⁻⁶	470	2.770	113	109	0.7691	76.91
	17 × 10 ⁻⁶	500	2.750	112	18	0.7708	77.08
	19 × 10 ⁻⁶	539	1.920	39	111	0.8400	84.00
	21 × 10 ⁻⁶	476	1.790	10	15	0.8508	85.08

3.3. Electrochemical impedance spectroscopy

The EIS provides important mechanistic and kinetic information for an electrochemical system under investigation. Fig. 7 show the Nyquist plots (a) and bode plots (b) for C-steel in 1 M HCl solution in the absence and presence of different concentrations of investigated organic compounds at 30°C. Nyquist impedance plots exhibits a single semi-circle shifted along the real impedance (Z_r). The Nyquist plots of compound (1) do not yield perfect semicircles as expected from the theory of EIS, the impedance loops measured are depressed semi-circles with their centers below the real axis, where the kind of phenomenon is known as the “dispersing effect” as a result of frequency dispersion [34] and mass transport resistant [35] as well as electrode surface heterogeneity resulting from surface roughness, impurities, dislocations, grain boundaries, adsorption of inhibitors, formation of porous layers [36–40], etc. so one constant phase element (CPE) is substituted for the capacitive element, to explain the depression of the capacitance semi-circle, to give a more accurate fit. Impedance data are analyzed using the circuit in Fig.8; in which R_s represents the electrolyte resistance, R_{ct} represents the charge-transfer resistance and the constant phase element (CPE). According to Hsu and Mansfeld [41] the correction of capacity to its real values is calculated from Eq. (7):

$$C_{dl} = Y_o (\omega_{max})^{n-1} \quad (7)$$

Where Y_o is the CPE coefficient, ω_{max} is the frequency at which the imaginary part of impedance ($-Z_i$) has a maximum and n is the CPE exponent (phase shift).

The data obtained from fitted spectra are listed in Table (7). The %IE was calculated from Eq. (8):

$$\% IE = \left(1 - \frac{R_{ct}^o}{R_{ct}} \right) \times 100 \quad (8)$$

Where R_{ct} and R_{ct}^o are the charge-transfer resistances with and without the inhibitors, respectively.

Data in Table 7 show that; the R_s values are very small compared to the R_{ct} values. Also; the R_{ct} values increase and the calculated C_{dl} values decrease by increasing the inhibitor concentrations, which causes an increase of θ and Y_i . The high R_{ct} values are generally associated with slower corroding system [42]. The decrease in the C_{dl} suggests that inhibitors function by adsorption at the metal/solution interface [43].

The inhibition efficiencies, calculated from EIS

results, show the same trend as those obtained from polarization measurements. The difference of inhibition efficiency from two methods may be attributed to the different surface status of the electrode in two measurements. EIS were performed at the rest potential, while in polarization measurements the electrode potential was polarized to high over potential, non-uniform current distributions, resulted from cell geometry, solution conductivity, counter and reference electrode placement, etc., will lead to the difference between the electrode area actually undergoing polarization and the total area [44].

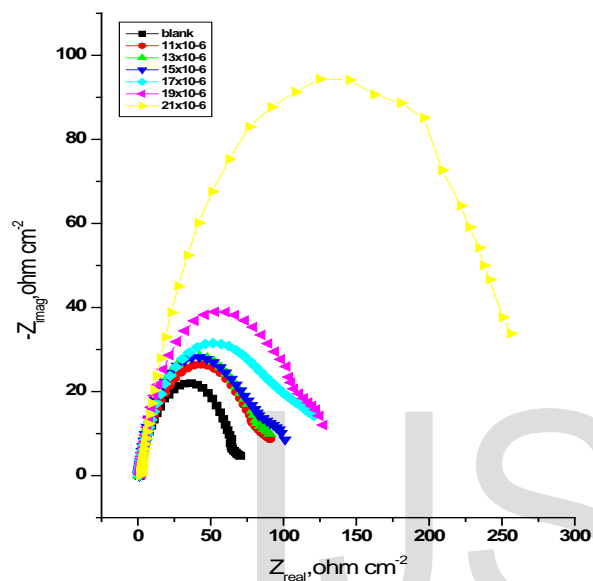


Fig. 7. The Nyquist (a) and Bode (b) plots for corrosion of C-steel in 1 M HCl in the absence and presence of different concentrations of compound (1) at 30°C.

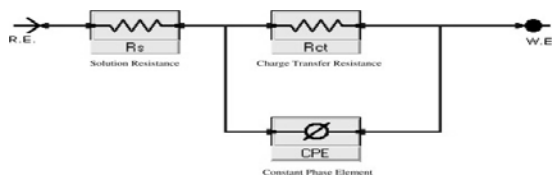


Fig. 8. The equivalent circuit model used to fit the experimental results

TABLE .7
ELECTROCHEMICAL KINETIC PARAMETERS OBTAINED BY EIS
TECHNIQUE FOR IN 1 M HCL WITHOUT AND WITH VARIOUS
CONCENTRATIONS OF COMPOUNDS AT 30°C

Comp.	Conc., M	R_s $\Omega \text{ cm}^2$	$Y_0 \times 10^{-3}$ $\mu\Omega^{-1} \text{ s/n}$	n	R_{ct} $\Omega \text{ cm}^2$	$C_{dl} \times 10^{-4}$ $\mu\text{F cm}^{-2}$	θ	% IE
1	Blank	8.572	362.3	0.7737	65.6	1.21	---	---
	11×10^{-6}	1.472	360.7	0.9419	375.7	2.47	0.825	82.5
	13×10^{-6}	1.295	355.0	0.7395	405.8	1.92	0.838	83.8
	15×10^{-6}	1.621	300.6	0.7986	406.2	1.77	0.839	83.9
	17×10^{-6}	1.518	249.0	0.8211	421.0	1.52	0.844	84.4
	19×10^{-6}	2.189	220.1	0.8251	476.8	1.37	0.862	86.2
2	21×10^{-6}	1.285	233.5	0.7549	762.5	1.33	0.914	91.4
	11×10^{-6}	1.266	357.3	0.7672	303.6	1.82	0.784	78.4
	13×10^{-6}	1.682	515.8	0.7483	318.5	2.80	0.794	79.4
	15×10^{-6}	1.182	321.9	0.8241	322.0	1.98	0.796	79.6
	17×10^{-6}	1.231	494.4	0.7391	336.8	2.63	0.805	80.5
	19×10^{-6}	3.323	381.0	0.755	345.1	1.977	0.809	80.9
3	21×10^{-6}	1.254	345.1	0.8256	348.7	2.21	0.812	81.2
	11×10^{-6}	8.490	279.7	0.8146	80.04	1.19	0.100	18.0
	13×10^{-6}	9.556	368.5	0.7749	81.58	1.33	0.196	19.6
	15×10^{-6}	9.996	418.2	0.8095	82.11	1.89	0.201	20.1
	17×10^{-6}	9.485	401.1	0.7599	101.8	1.46	0.356	35.5
	19×10^{-6}	2.091	353.5	0.8126	111.9	1.68	0.414	41.4

3.4. Electrochemical Frequency Modulation Measurements

Bosch et al. recently proposed electrochemical frequency modulation (EFM) as a new electrochemical technique for online corrosion monitoring [45-48]. EFM is a rapid and nondestructive corrosion rate measurement technique that can directly give values of the corrosion current without prior knowledge of Tafel constants.

In corrosion research, it is known that the corrosion process is non-linear in nature, a potential distortion by one or more sine waves will generate responses at more frequencies than the frequencies of applied signal. Virtually no attention has been given to the intermodulation or electrochemical frequency modulation. However, EFM showed that this non-linear response contains enough information about the corroding system so that the corrosion current can be calculated directly. The great strength of the EFM is the causality factors which serve as an internal check on the validity of the EFM measurement. With the causality factors the experimental EFM data can be verified.

Fig. 9 show the current response contains not only the input frequencies, but also contains frequency components which are the sum, difference, and multiples of the two input frequencies.

The electrochemical corrosion kinetic parameters at different concentrations of inhibitors in 1 M HCl at 30°C were shown in Table (8). The inhibition efficiency was found to increase with increasing the inhibitor concentrations. The causality factors CF-2 and CF-3 in Table 8 are close to their theoretical values of 2.0 and 3.0, respectively indicating that the measured data are of good quality.

The calculated inhibition efficiency obtained from weight loss, Tafel polarization and EIS measurements are in good agreement with that obtained from EFM measurements.

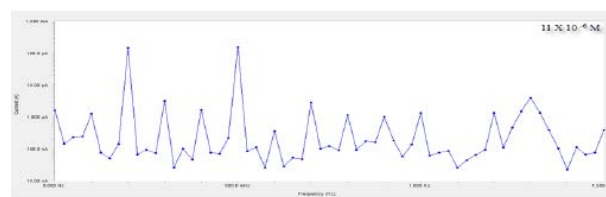
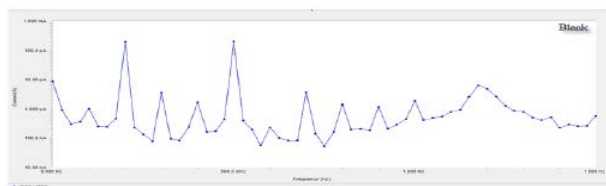


TABLE. 8

ELECTROCHEMICAL KINETIC PARAMETERS OBTAINED BY EFM TECHNIQUE FOR C-STEEL IN THE ABSENCE AND PRESENCE OF VARIOUS CONCENTRATIONS OF INHIBITORS (1-3) IN 1M HCL AT 30°C

Comp.	Conc., M	i_{cor} μA cm^{-2}	β_c $mV dec^{-1}$	β_a $mV dec^{-1}$	CF-2	CF-3	CR	θ	% IE
1	Blank	355.4	121.0	107.0	2.03	3.01	162.4	---	---
	11×10^{-6}	62.7	134.1	105.0	1.85	2.32	30.98	0.823	82.3
	13×10^{-6}	60.5	106.9	103.6	2.05	2.99	27.9	0.830	83.0
	15×10^{-6}	59.5	110.0	75.4	2.03	2.46	27.42	0.833	83.3
	17×10^{-6}	56.8	74.6	70.6	2.05	3.92	25.82	0.841	84.1
	19×10^{-6}	46.6	66.5	58.3	2.19	2.97	21.47	0.869	86.9
2	21×10^{-6}	38.2	126.2	109.3	1.79	2.93	18.88	0.892	89.2
	11×10^{-6}	93.5	192.3	147.9	2.19	3.06	46.18	0.737	73.7
	13×10^{-6}	85.2	103.2	90.6	2.19	3.07	39.28	0.760	76.0
	15×10^{-6}	84.8	123.0	97.2	2.16	3.12	39.08	0.761	76.1
	17×10^{-6}	80.5	131.2	103.4	2.19	3.08	39.76	0.773	77.3
	19×10^{-6}	75.5	127.3	104.2	1.76	2.13	37.27	0.787	78.7
3	21×10^{-6}	73.7	138.3	107.9	1.53	2.35	36.38	0.793	79.3
	11×10^{-6}	299.3	141.1	120.1	1.98	3.16	136.8	0.158	15.8
	13×10^{-6}	298.5	125.1	120.6	2.14	3.65	136.4	0.160	16.0
	15×10^{-6}	288.5	153.3	146.2	2.07	3.62	131.8	0.188	18.8
	17×10^{-6}	254.7	166.1	120.0	2.02	3.06	116.4	0.283	28.3
	19×10^{-6}	244.1	110.2	91.2	1.91	3.07	111.5	0.313	31.3
	21×10^{-6}	152.9	319.1	147.7	2.04	2.84	70.44	0.570	57.0

3.5- SCANNING ELECTRON MICROSCOPY (SEM) STUDIES

Figure (10) represents the micrography obtained for C-steel samples in presence and in absence of 21×10^{-6} M thiourea derivatives after exposure for 3 days immersion. It is clear that C-steel surfaces suffer from severe corrosion attack in the blank sample. It is important to stress out that when the compound is present in the solution, the morphology of C-steel surfaces is quite different from the previous one, and the specimen surfaces were smoother. We noted the formation of a film which is distributed in a random way on the whole surface of the carbon steel. This may be interpreted as due to the adsorption of the thiourea derivatives on the C-steel surface incorporating into the passive film in order to block the active site present on the C-steel surface. Or due to the involvement of inhibitor molecules in the interaction with the reaction sites of C-steel surface, resulting in a decrease in the contact between C-steel and the aggressive medium and sequentially exhibited excellent inhibition effect [49, 50].



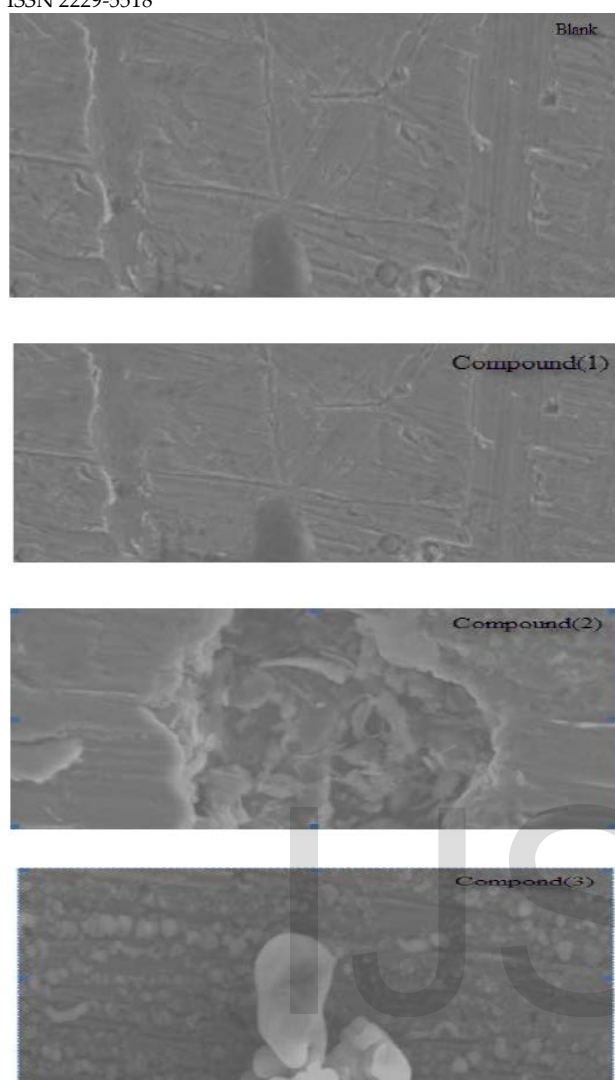


Fig.10. SEM images of C-steel in 1 M HCl solution after immersion for 3 days without inhibitor and in presence of 21×10^{-6} M of thiourea derivatives.

3.6. Energy Dispersion Spectroscopy (EDS) Studies

The EDS spectra were used to determine the elements present on the surface of C-steel and after 3 days of exposure in the uninhibited and inhibited 1 M HCl. Fig. 11 shows the EDS analysis result on the composition of C-steel only without the acid and inhibitor treatment. The EDS analysis indicates that only Fe and oxygen were detected, which shows that the passive film contained only Fe_2O_3 . Fig. 11 portrays the EDS analysis of C-steel in 1 M HCl only and in the presence of 21×10^{-6} M of thiourea derivatives. The spectra show additional lines, demonstrating the existence of C (owing to the carbon atoms of thiourea derivatives). These data shows that the carbon and O atoms covered the specimen surface. This layer is entirely owing to the inhibitor, because the carbon and O signals are absent on the specimen surface exposed

to uninhibited HCl. It is seen that, in addition to Mn, C. and O were present in the spectra. A comparable elemental distribution is shown in Table (9).

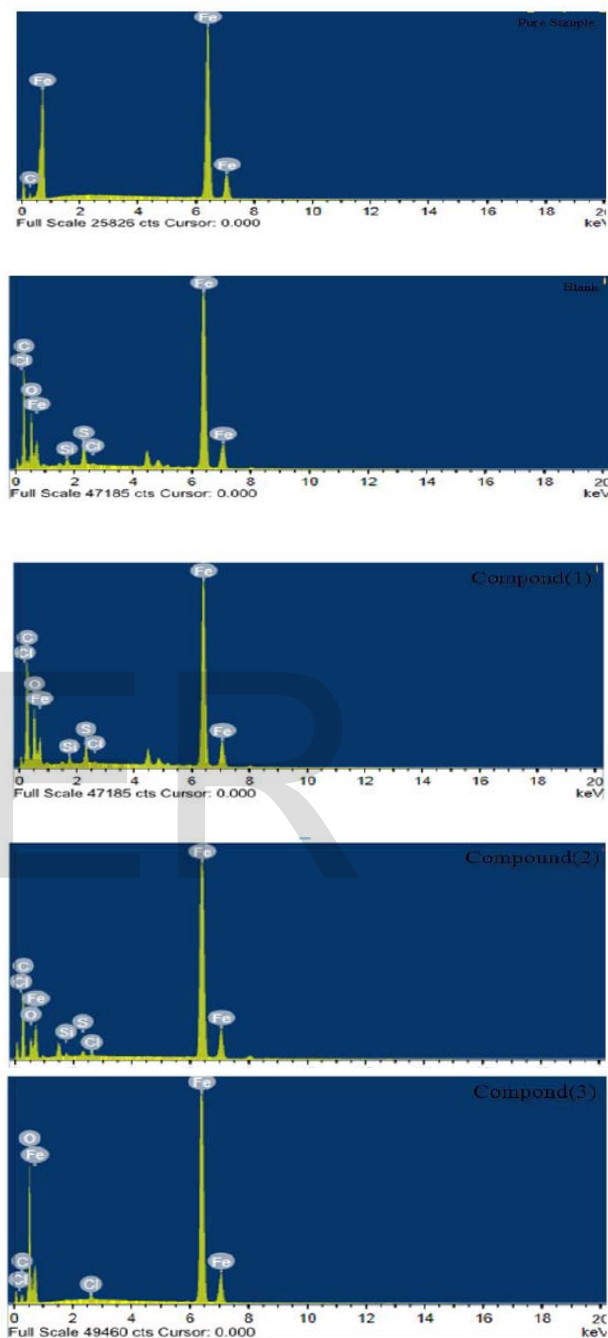


Fig.11. EDS analysis of C-steel in 1 M HCl solution after immersion for 3 days without inhibitor and in presence of 21×10^{-6} M of thiourea derivatives.

TABLE.9

SURFACE COMPOSITION (WEIGHT %) OF C-STEEL AFTER 3HRS OF IMMERSION IN HCL WITHOUT AND WITH THE OPTIMUM CONCENTRATIONS OF THE STUDIED INHIBITORS

(Mass %)	Fe	C	O	Cl	S	Si
Pure	92.16	7.84	--	--	--	--
Blank	21.36	9.23	17	0.35	0.06	0.39
Compound (1)	64.46	50.61	27.75	0.12	1.03	0.37
Compound (2)	47.91	19.68	15.55	0.21	0.32	1.49
Compound (3)	43.04	9.69	16.91	0.32	0.01	0.32

Theoretical calculations were performed for only the neutral forms, in order to give further insight into the experimental results. Values of quantum chemical indices such as energies of LUMO and HOMO (E_{HOMO} and E_{LUMO}), the formation heat ΔH_f and energy gap ΔE , are calculated by semi-empirical AM1, MNDO and PM3 methods has been given in Table 10. The reactive ability of the inhibitor is related to E_{HOMO} , E_{LUMO} [51]. Higher E_{HOMO} of the adsorbent leads to higher electron donating ability [52]. Low E_{LUMO} indicates that the acceptor accepts electrons easily. The calculated quantum chemical indices (E_{HOMO} , E_{LUMO} , μ) of investigated compounds are shown in Table (10). The difference $\Delta E = E_{\text{LUMO}} - E_{\text{HOMO}}$ is the energy required to move an electron from HOMO to LUMO. Low ΔE facilitates adsorption of the molecule and thus will cause higher inhibition efficiency.

The bond gap energy ΔE increases from (1 to 3). This fact explains the decreasing inhibition efficiency in this order ($1 > 2 > 3$), as shown in Table 10 and Fig. 12 show the optimized structures of the three investigated compounds. So, the calculated energy gaps show reasonably good correlation with the efficiency of corrosion inhibition. Table (10) also indicates that compound (1) possesses the lowest total energy that means that compound (1) adsorption occurs easily and is favored by the highest softness. The HOMO and LUMO electronic density distributions of these molecules were plotted in Fig. 12. For the HOMO of the studied compounds that the benzene ring, N-atoms and O-atom have a large electron density. The data presented in Table. 10 show that the calculated dipole moment decrease from ($1 > 2 > 3$).

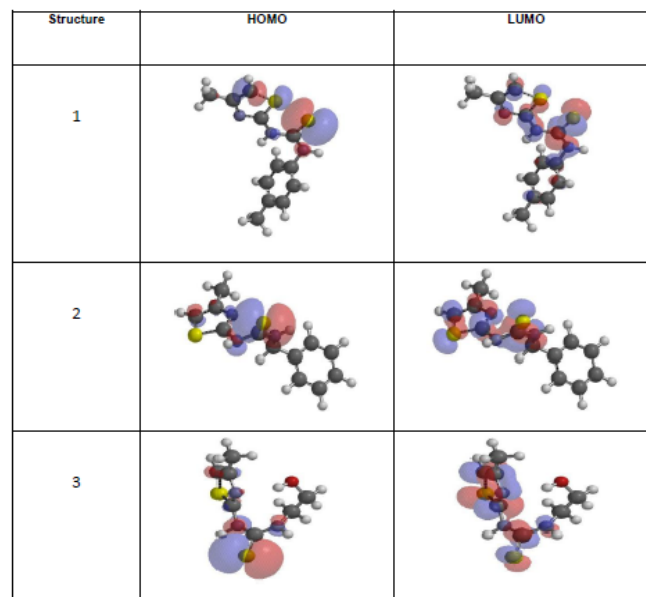


Fig.12. Molecular orbital plots and Mulliken charges of investigated compounds

TABLE .10

THE CALCULATED QUANTUM CHEMICAL PROPERTIES FOR INVESTIGATED COMPOUNDS

	Compound (1)	Compound (2)	Compound (3)
-E _{HOMO} (eV)	8.42	8.71	8.78
-E _{LUMO} (eV)	1.21	1.02	0.73
ΔE (eV)	7.21	7.69	8.05
I_f (eV)	3.605	3.845	4.025
σ (eV ⁻¹)	0.277	0.260	0.246
-Pi (eV)	4.815	4.865	4.755
χ (eV)	4.815	4.865	4.755
Dipole moment (Debye)	5.67	5.90	4.28
Area (Å ²)	277.74	285.72	230.26

3.8. Inhibition Mechanism

Inhibition of the corrosion of C-steel in 1 M HCl solution by investigated thiourea derivatives is determined by weight loss, potentiodynamic polarization measurements, electrochemical impedance spectroscopy (EIS), and electrochemical frequency modulation method (EFM), it was found that the inhibition efficiency depends on concentration, nature of metal, the mode of adsorption of the inhibitors and surface conditions. The adsorption of inhibitor depends on its concentration. As shown in Figure (13), at adsorption density less than a monolayer (Fig. 13. a), most of the nucleation sites are still possibly exposed to HCl, since inhibitor adsorbs less likely on them. When the adsorption

density reaches monolayer adsorption (Fig. 13.b), some of the nucleation sites begin to be covered by inhibitor molecules. At maximum adsorption density (Fig.13. c), the inhibitor molecules cover the whole surface, including the nucleation sites, and then complete inhibition occurs.

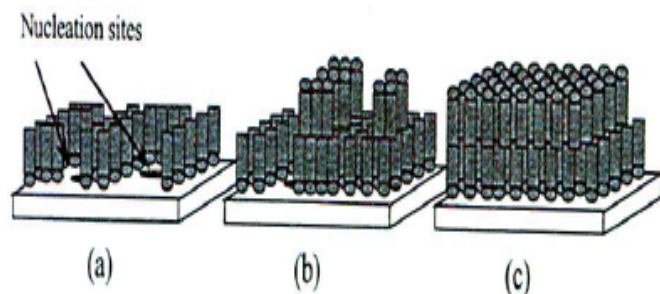


Fig.13. Adsorption schemes for organic additives as inhibitors at:
(a) Low concentration,
(b) intermediate concentration, (c) high concentration on copper

The observed corrosion data in presence of these inhibitors, namely:

i) The decrease of corrosion rate and corrosion current with increase in concentration of the inhibitor.
ii) The linear variation of weight loss with time. iii) The shift in Tafel lines to higher potential regions. iv) The decrease in corrosion inhibition with increasing temperature indicates that desorption of the adsorbed inhibitor molecules takes place and v) the inhibition efficiency was shown to depend on the number of adsorption active centers in the molecule and their charge density.

The corrosion inhibition is due to adsorption of the inhibitors at the electrode/solution interface, the extent of adsorption of an inhibitor depends on the nature of the metal, the mode of adsorption of the inhibitor and the surface conditions. Adsorption on C-steel surface is assumed to take place mainly through the active centers attached to the inhibitor and would depend on their charge density. Transfer of lone pairs of electrons on the nitrogen atoms to the C-steel surface to form a coordinate type of linkage is favored by the presence of a vacant orbital in iron atom of low energy. Polar character of substituents in the changing part of the inhibitor molecule seems to have a prominent effect on the electron charge density of the molecule.

It was concluded that the mode of adsorption depends on the affinity of the metal towards the π -electron clouds of the ring system. Metals such as Cu and Fe which have a greater affinity towards aromatic moieties were found to adsorb benzene rings in a flat orientation. The order of decreasing the inhibition efficiency of the investigated inhibitors in the corrosive solution was as follows: compound (1) > compound (2) > compound (3)

Compound (1) exhibits excellent inhibition

power due to: (i) its larger molecular size that may facilitate better surface coverage, and (ii) its adsorption through six active centers. Compound (2) comes after compound (1) in inhibition efficiency due to its lower molecular size than compound (1). Compound (3) comes after compound (2) in inhibition efficiency because it has lower molecular size than compound (2).

4. CONCLUSIONS

- The thiourea derivatives inhibit the corrosion of C-steel in 1 M HCl.
- The inhibition is due to adsorption of the thiourea derivatives on the C-steel surface by blocking its active sites.
- Adsorption of thiourea derivatives fits Temkin isotherm.
- Results obtained from weight loss, DC polarization, and AC impedance techniques are reasonably in good agreement and show increased inhibitor efficiency with increasing inhibitor concentration.
- Polarization data showed that the used inhibitors act as mixed-type inhibitor in 1 M HCl.
- The results of EIS revealed that an increase in the charge transfer resistance and a decrease in double layer capacitances when the inhibitor is added and hence an increase in % IE. This is attributed to increase of the thickness of the electrical double layer
- The morphology of inhibited and uninhibited C-steel was analyzed by scanning electron microscope (SEM) and energy dispersive X-ray spectroscopy (EDX).
- The order of % IE of these investigated compounds is in the following order: compound (1) > compound (2) > compound (3)
- The values of E_{HOMO} and E_{LUMO} decreases in an order runs parallel to the increase in % IE obtained which support the previous order

5. REFERENCES

- [1] M. A. Deyab, *corros. Sci.* 49 (2007) 2315-2328
- [2] S.A. Abd El-Maksoud A.S. Fouda, *Mater. Chem. phys.* 93(2005) 84-90
- [3] K. F. Khaled, *Mater. Chem. phys.* 122(2008) 290-300
- [4] E. Machnikova, K. H. Whitmire and N Hackeman, *Electrochim. Acta* 53 (2008) 6024-6032
- [5] H Ashassi-sorkhabi, M. R. Magidi and K. Seyyedi, *Appt. Surf. Sci.* 225 (2004) 176-185
- [6] M. A. Migahed and I.F. Nasser, *Electrochim. Acta* 53 (2008) 2877- 2882
- [7] G. Avci, *Colloids Surf. A* 317 (2008) 730-736
- [8] K. C. Pillali and R. Narayan, *Corros. Sci.*, 23(1985)151
- [9] A. B. Tados and B. A. Abdel-Naby, *J. Electroanal. Chem.*, 224 (1988) 433.
- [10] JO' M. Bockris and B. Yang, *J. Electrochem.*, 138 (1991) 2237.

- [11] V. Jovancicevic, B. Yang and J. O'M. Bockris, *J. Electrochem. Soc.*, 135 (1989) 94
- [12] J. Uhera and K. Aramaki, *J. Electrochem. Soc.*, 138 (1991) 3245.
- [13] A. A. Akust, W. J. Lorenz and F. Mansfeld, *Corros. Sci.*, 22 (1982) 611.
- [14] M. Abdallah, E. A. Helal and A. S. Fouda, *Corros. Sci.*, 48 (2006) 1639-1654.
- [15] A. S. Fouda, A. A. Al-Sarawy and E. E. El-Katori, *Chem. Paper*, 60 (1) (2006) 5-9.
- [16] A. S. Fouda, A. A. Al-Sarawy and E. E. El-Katori, *Desalination J.*, 201 (2006) 1-13.
- [17] O. Benali, L. Larabi, M. Traisnel, L. Gengembra, Y. Harwk, *Appl. Surf. Sci.* 253(2007)6130-6139.
- [18] M.A. Khalifa, M. El-Batouti, F. Mhgoub, A. Bakr Aknish, *Mater. Corrps.* 54 (2003) 251-258.
- [19] Y. Abboud, A. Abourriche, T. Saffag, M. Berrada, M. Charrouf, A. Bennamara, N. Al Himidi and H. Hannache, *Mater. Chem. phy.* 105 (2007) 1-5.
- [20] K. F Khaled, *Electrochim. Acta* 48 (2003) 2493-2503
- [21] A. Popova M. Chistov, S. Raicheva and E. Sokolova, *Corros. Sci* 46 (2004) 1333-1350.
- [22] C. Alkan, K. Kaya and A. Sari, *J. Mater. Lett.* 62 (2008) 1122-1125.
- [23] Y. A. El-Awady, A. K. Mohamed, A. A. El-Shafei and M. Abo El-Wafa, *Bull. Electrochem.*, 17 (17) (2001) 145 .
- [24] F. Bensajjay, S. Alehyen, M. El Achouri, S. Kertit, *Anti-Corros. Meth. Mater.* 50 (2003) 402.
- [25] S. Z. Duan, Y. L. Tao, *Interface Chem. Higher Education Press, Beijing*, (1990) 124.
- [26] S. S. Abd El-Rehim, S. A. M. Refaey, F. Taha, M. B. Saleh, R. A. Ahmed, *J. Appl. Electrochem.* 31 (2001) 429.
- [27] I. N. Putilova, S. A. Balezin, V. P. Barannik, *Metallic Corrosion Inhibitors*, Pergamon Press, New York, (1960) 31.
- [28] K. K. Al-Neami, A. K. Mohamed, I. M. Kenawy, A. S. Fouda, *Monatsh Chem.*, 126 (1995) 369.
- [29] E. A. Noor, *Int. J. Electrochem. Sci.*, 2 (2007) 996-1017.
- [30] J. Marsh, *Advanced Organic Chemistry*, 3rd ed, Wiley Eastern, New Delhi, (1988).
- [31] S. Martinez, *Appl. Surf. Sci.*, 199 (2002) 83.
- [32] R. T. Vashi, V. A. Champaneri, *Indian J. Chem. Technol.* (1997) 180.
- [33] A. K. Mohamed, H. A. Mostafa, G. Y. El-Awady, A. S. Fouda, *Port. Electrochim. Acta* 18 (2000) 99.
- [34] M. El Achouri, S. Kertit, H. M. Gouttaya, B. Nciri, Y. Bensouda, L. Perez, M. R. Infante and K. Elkacemi, *Prog. Org. Coat.*, 43 (2001) 267.
- [35] K. F. Khaled, *Electrochim. Acta*, 48 (2003) 2493.
- [36] F. B. Growcock and J. H. Jasinski, *J. Electrochem. Soc.*, 136 (1989) 2310.
- [37] U. Rammet and G. Reinhart, *Corros. Sci.*, 27 (1987) 373.
- [38] A. H. Mehaute and G. Grepy, *Solid State Ionics* 9-10 (1983) 17.
- [39] E. Machnikova, M. Pazderova, M. Bazzaoui and N. Hackerman, *Surf. Coat. Technol.*, 202 (2008) 1543.
- [40] C. H. Hsu and F. Mansfeld, *Corrosion* 57 (2001) 747.
- [41] M. Lebrini, M. Lagrenée, M. Traisnel, L. Gengembre, H. Vezin and F. Bentiss, *Appl. Surf. Sci.*, 253 (2007) 9267.
- [42] R. W. Bosch, J. Hubrecht, W. F. Bogaerts and B. C. Syrett, *Corrosion*, 57 (2001) 60.
- [43] Gamry Echem Analyst Manual, (2003).
- [44] R. G. Kelly, J. R. Scully, D. W. Shoesmith and R. G. Buchheit, *Electrochemical Techniques in Corrosion Science and Engineering*, Marcel Dekker, Inc., New York, (2002) 148.
- [45] R. W. Bosch, J. Hubrecht, W. F. Bogaerts, B. C. Syrett, *Corrosion*, 57 (2001) 60.
- [46] K. F. Khaled, *Int. J. Electrochem. Sci.* 3 (2008) 462.
- [47] K. F. Khaled, *Electrochim. Acta* 53 (2008) 3484.
- [48] D. A. Jones, *Principles and Prevention of Corrosion*, second ed., Prentice Hall, Upper Saddle River, NJ, (1983).
- [49] R. A., Prabhu, T. V., Venkatesha, A. V., Shanbhag, G. M., Kulkarni, R. G., *Kalkhambkar, Corros. Sci.*, 50 (2008) 3356
- [50] G., Moretti, G., Quartanone, A., Tassan, A., Zingales, *Wkst. Korros.*, 45 (1994) 641
- [51] C. Lee, W. Yang and R. G. Parr, *Phys. Rev. B*, 37 (1988) 785.
- [52] R. M. Issa, M. K. Awad and F. M. Atlam, *Appl. Surf. Sci.*, 255 (2008) 2433